Research Square

Preprints are preliminary reports that have not undergone peer review.
They should not be considered conclusive, used to inform clinical practice,
or referenced by the media as validated information.

Integrated biological and chemical strategies for sustainable management of Nigrospora coryli-induced tobacco leaf spot

Jingpei Zou
Liuti Cai
Yiming Geng
Mengyu Yin
Yuguang Mu
Jingjing Guo
Hancheng Wang
Feng Zhang
fengz@njau.edu.cn

Research Article

Keywords: Tobacco leaf spot, Nigrospora coryli, biological characterization, phyllosphere microbial community, biocontrol, fungicide synergy

Posted Date: April 28th, 2026

DOI: https://doi.org/10.21203/rs.3.rs-9462624/v1

License: This work is licensed under a Creative Commons Attribution 4.0 International License.
Read Full License

Additional Declarations: No competing interests reported.

Version of Record: A version of this preprint was published at Archives of Microbiology on July 21st, 2026. See the published version at https://doi.org/10.1007/s00203-026-05056-5.

Integrated biological and chemical strategies for sustainable management of *Nigrospora coryli*-induced tobacco leaf spot

Jingpei Zou[1, 2], Liuti Cai[1, 2], Yiming Geng[1], Mengyu Yin[1], Yuguang Mu[4], Jingjing Guo[5], Hancheng Wang[2, *], Feng Zhang[1, 3, *]

[1] State Key Laboratory of Agricultural and Forestry Biosecurity, College of Plant Protection, Nanjing Agricultural University, Nanjing, 210095, China.

[2] Guizhou Provincial Academician Workstation of Microbiology and Health, Guizhou Academy of Tobacco Science, Guiyang 550081, China.

[3] Sanya Institute, Nanjing Agricultural University, Sanya 572025, China.

[4] School of Biological Sciences, Nanyang Technological University, Singapore, Singapore.

[5] Centre for Artificial Intelligence Driven Drug Discovery, Faculty of Applied Sciences and Engineering Research Centre of Applied Technology on Machine Translation and Artificial Intelligence, Macao Polytechnic University, Macao 999078, China.

[2] These authors contributed equally to this article.

[*] Corresponding authors.

Email addresses: fengz@njau.edu.cn (Feng Zhang), xiaobaiyang126@hotmail.com (Hancheng Wang).

Abstract

Tobacco (*Nicotiana tabacum*) leaf spot disease caused by fungal pathogens poses a major threat to crop yield and quality worldwide. Recently, *Nigrospora coryli* was identified as a novel causal agent of tobacco leaf spot in China, yet its biology, ecological interactions, and management strategies remained largely unexplored. In this study, we systematically characterized *N. coryli* through growth physiology, environmental adaptability, phyllosphere microbiome profiling, microbial interactions, and fungicide sensitivity assays. The pathogen exhibited robust environmental tolerance, with optimal growth at 28°C and pH 6.0, viability across pH 4–11, and survival at temperatures up to 57°C, while preferring soluble starch and peptone as nutrient sources. High-throughput sequencing revealed disease-associated phyllosphere shifts, including enrichment of Stenotrophomonas and Pseudomonas in symptomatic leaves and the exclusive detection of *Nigrospora* and *Sarocladium* in diseased tissues. Functional screening identified multiple antagonistic microbes, with *Aspergillus niger* MGM reducing lesion size by 87.6% in planta, while *Pseudomonas syringae* pv. *angulata* SLB-5-3 exacerbated disease. Among eight commercial fungicides, fludioxonil was the most potent (EC_{50} = 0.0057 μg/mL), followed by the prochloraz-manganese chloride complex, difenoconazole, and fenaminstrobin. Synergistic interactions were observed in binary mixtures: fludioxonil + difenoconazole (1:4, SR = 1.7360), fludioxonil + fenaminstrobin (1:1, SR = 1.5365), and difenoconazole + fenaminstrobin (1:2, SR = 2.0219). These findings highlight the potential of integrating potent biocontrol agents with synergistic fungicide combinations for sustainable management of *N. coryli*-induced tobacco leaf spot. This study provides a comprehensive foundation for developing environmentally sound, multifaceted disease control strategies.

Keywords: Tobacco leaf spot, *Nigrospora coryli*, biological characterization, phyllosphere microbial community, biocontrol, fungicide synergy

Tobacco (*Nicotiana tabacum*) is a globally important cash crop, with its leaves serving as a primary raw material for cigarette production (Gui et al. 2024). Beyond its economic significance, tobacco also possesses pharmacological potential, with applications in pesticides, tranquilizers, and anesthetics (Le Foll et al. 2022). Globally, approximately 33 million people are involved in tobacco cultivation, processing, distribution, and retail, contributing to an estimated annual income of $2 trillion (Warner 2000; Martins-da-Silva et al. 2022).

However, tobacco leaves exhibit high susceptibility to fungi pathogens throughout their growth cycle, resulting in severe foliar diseases and substantial economic losses (Huang et al. 2025). Several major pathogens, including species from genera *Corynespora*, *Didymella*, *Fusarium*, and *Nigrospora*, have been consistently isolated from leaf spot lesions (Huang et al. 2021; Feng et al. 2024; Tao et al. 2024). Among these, *Nigrospora* species have emerged as significant pathogens, causing leaf spots, causing twig and shoot blight or rot on a wide range of economically important crops worldwide (Chen et al. 2022). *Nigrospora*, a diverse genus of ascomycetous fungi in the family Apiosporaceae (Xylariales, Sordariomycetes), is notable for its ability to colonize numerous terrestrial and aquatic plant species (Hao et al. 2020; Xu et al. 2022). The genus was first described by Zimmerman in 1902 as the endophytic fungus *Nigrospora panici* from *Panicum amphibium* leaves (Wang et al. 2017). Previously, *Nigrospora oryzae* was the only species reported to cause disease on legumes in China, including leaf spot on kidney bean (*Phaseolus vulgaris* L.) (Luo and Jiang 2022). In our previous study, *Nigrospora coryli* was identified as a novel causal agent of tobacco leaf spot in China, with field incidences reaching 41–47% in severely affected areas (Zou et al. 2026). Despite this, the pathogen's biological characteristics and effective management strategies remain unknown.

Understanding the biology and environmental adaptability of a pathogen is essential for predicting disease outbreaks and developing effective control measures(De Wolf and Isard 2007). The phyllosphere, the aerial surface of plants, harbors complex microbial communities, including bacteria and fungi, which play crucial roles in plant health and disease dynamics (Stone et al. 2018). These communities can directly interact with pathogens through competition, antagonism, or synergism, thereby influencing disease outcomes. Moreover, integrating chemical and biological control strategies offers promising avenues for sustainable disease management. Identifying effective fungicides and synergistic combinations can reduce chemical inputs and delay resistance development (Ons et al. 2020).

In this study, we comprehensively characterized the growth physiology, environmental adaptability, and nutrient preferences of *N. coryli*. High-throughput sequencing was used to analyze the composition and diversity of phyllosphere microbial communities on both asymptomatic and symptomatic leaves. *In vitro* plate confrontation assays and *in planta* co-infection assays were employed to identify dominant phyllosphere microorganisms with biocontrol potential against *N. coryli*. Additionally, we evaluated the inhibitory effects of eight commercial fungicides representing different chemical classes and modes of action. The four most effective fungicides were further combined in binary mixtures to identify synergistic interactions that enhance efficacy while minimizing fungicide use. This integrated approach establishes a foundation for sustainable, multifaceted management strategies against *Nigrospora*-induced tobacco leaf spot disease.

2. Materials and Methods

2.1. Strain and culture condition

N. coryli strain YB13 was originally isolated from symptomatic leaves of tobacco (*Nicotiana tabacum* cv. Yunyan 87) at seedling stage (four to five leaves) collected in Zhengan (107.43° N, 28.55° E), Guizhou Province, China, in June 2025. In our previous study, YB13 was molecularly identified as *N. coryli* through multilocus phylogenetic analysis and confirmed as pathogenic to tobacco (Zou et al. 2026). The GenBank accession numbers for the marker genes are *ITS*: PX736263, *GAPDH*: PX556631, *TUB2*: PX556632, and *TEF1-α*: PX711191. Based on its confirmed pathogenicity and taxonomic status, YB13 was selected as the representative strain for subsequent biological characterization and biocontrol assays in the present study. The bacterial and fungal strains used in the plate confrontation and co-inoculation assays were isolated from symptomatic tobacco leaves collected from the same fields and at the same growth stage as YB13. These phyllosphere microbial strains were kindly provided by the Guizhou Province Tobacco Research Institute. Detailed information on each strain is listed in Table S1. All strains used in this study were cultured on various agar media including potato dextrose agar (PDA), alkyl ester agar (AEA), czapek dox agar (CDA) and oatmeal agar (OA). All reagents were obtained from commercial biological reagent suppliers and stored at 2–8°C until use.

2.2. Growth characteristics of N. coryli

To characterize the growth of *N. coryli*, the effects of culture medium and environmental factors including temperature, pH, carbon source, nitrogen source, and light conditions on the biological traits of the isolate YB13 were investigated.

Optimal growth medium was determined by inoculating mycelial plugs onto PDA, AEA, and OA. Plates were sealed with Parafilm® and incubated at 28 °C. Colony diameter was measured after 14 days. To clarify the effect of temperature on mycelial growth, the isolate YB13 was cultured on PDA medium for 7 days. Using a sterilized 5-mm inner diameter punch, PDA plugs containing

mycelia were cut from the edge of the colonies and inoculated onto the center of fresh PDA plates. The plates were then incubated in darkness at four temperature gradients: 20°C, 25°C, 28°C, and 30°C. Lethal temperature was determined by immersing plugs in sterile water at 35–60 °C for 10 min, cooling immediately, and then incubating on PDA at 28 °C for 7 days. The lethal range was refined at 1 °C intervals. Mycelial growth characteristics under varying pH conditions were investigated. 1 M HCl and 1 M NaOH solutions were used to adjust the pH of the PDA medium to levels ranging from 4 to 11, resulting in eight distinct pH gradients. Plugs were inoculated and incubated at 28 °C in darkness. After 14 days, colony diameters were measured. Light response was evaluated under constant light (LL), constant darkness (DD), or a 12 h light/dark cycle (LD) in an artificial climate chamber (Model QHX-1000, Wuhan Greenfafa Institute of Novel Genechip R&D Co., Ltd., Wuhan, China) at 28 °C. The light source used was cool-white fluorescent lamps, which are the default lighting configuration of the chamber. Colony diameter was measured after 14 days of incubation. Carbon and nitrogen utilization was tested on CDA supplemented with individual carbon sources (soluble starch, glucose, sucrose, maltose, sorbitol) or nitrogen sources (sodium nitrate, peptone, glycine, alanine, urea). These compounds were selected based on their prevalence in plant tissues. Mycelial plugs were taken from the edge of the *N. coryli* YB13 colony using a sterile cork borer and inoculated at the center of CDA plates supplemented with the respective carbon or nitrogen sources. Cultures were incubated at 28 °C for 14 days, with CDA medium lacking both carbon and nitrogen sources serving as the control. Colony diameters were then recorded. Each treatment was performed in triplicate to ensure statistical reliability.

2.3. DNA extraction and 16S rRNA gene sequencing

To examine shifts in the phyllosphere microbial assemblage associated with *N. coryli* infection and to identify candidate antagonists for biocontrol development, we profiled bacterial and fungal

communities on tobacco leaves via high-throughput amplicon sequencing. Tobacco leaves (cv. Yunyan 87) at the four-to-five-leaf stage were collected from field-grown plants displaying either typical leaf spot symptoms or appearing asymptomatic. For each group, three independent biological replicates were obtained, with each replicate consisting of leaves pooled from five individual plants. Samples were flash-frozen in liquid nitrogen immediately after collection and preserved at −80°C until processing. Total genomic DNA was extracted from 0.5 g of leaf tissue per sample using the cetyltrimethylammonium bromide (CTAB) method (Clarke 2009). DNA integrity and purity were evaluated via 1% agarose gel electrophoresis and spectrophotometric analysis (NanoDrop 2000, Thermo Scientific, USA). An appropriate amount of DNA was diluted with sterile water to a concentration of 1 ng/μL, and 1 μL of this diluted DNA (1 ng total) served as the template for PCR amplification. For bacterial community analysis, the V3-V4 hypervariable region of the 16S rRNA gene was amplified using primers 338F (5'-ACTCCTACGGGAGGCAGCAG-3') and 806R (5'-GGACTACHVGGGTWTCTAAT-3') (Shi et al. 2023). For fungal community analysis, the internal transcribed spacer (ITS) region was amplified using primers ITS1 (5'-TCCGTAGGTGAACCTGCGG-3') and ITS4 (5'-TCCTCCGCTTATTGATATGC-3') (O'Brien et al. 2005). PCR reactions (20 μL each) were run in triplicate and contained 1× PCR buffer, 0.2 mM dNTPs, 0.2 μM each primer, 1 U of Phusion High-Fidelity DNA Polymerase (New England Biolabs, USA), and 10 ng of template DNA. Thermal cycling conditions consisted of initial denaturation at 98°C for 1 min, followed by 30 cycles of 98°C for 10 s, 50°C (for bacteria) or 55°C (for fungi) for 30 s, and 72°C for 30 s, with a final extension at 72°C for 5 min. PCR products were pooled per sample and purified using a GeneJET Gel Extraction Kit (Thermo Scientific, USA). Sequencing libraries were prepared using the NEB Next Ultra DNA Library Prep Kit for Illumina (New England Biolabs, USA) according

to the manufacturer's instructions. Library concentration and fragment size distribution were assessed with a Qubit 2.0 Fluorometer (Thermo Scientific, USA) and an Agilent 2100 Bioanalyzer (Agilent Technologies, USA). Paired-end sequencing (2 × 250 bp) was performed on an Illumina NovaSeq 6000 platform by Novogene Bioinformatics Technology Co., Ltd. (Beijing, China).

Raw sequencing data were demultiplexed and quality-filtered using QIIME2 (version 2020.11) (Bolyen et al. 2019). The DADA2 plugin was employed for denoising, chimera removal, and inference of amplicon sequence variants (ASVs) (Callahan et al. 2016). Taxonomic assignment of bacterial ASVs was performed against the SILVA database (release 138) (Chuvochina et al. 2026) with an 80% confidence threshold, while fungal ASVs were classified using the UNITE database (version 9.0) (Abarenkov et al. 2024). The sequencing generated 470,985 raw reads, which after quality filtering and chimera removal yielded 334,621 high-quality sequences for downstream analysis (Table S2).

Additionally, to confirm the identity of culturable microbial strains used in subsequent antagonism assays, individual fungal and bacterial isolates were subjected to Sanger sequencing. For fungal isolates, genomic DNA was extracted from mycelia using the CTAB method (Clarke 2009), and the ITS region was amplified with primers ITS1/ITS4 as described above (O'Brien et al. 2005). For bacterial isolates, the 16S rRNA gene was amplified with primers 27F (5'-AGAGTTTGATCMTGGCTCAG-3') and 1492R (5'-GGTTACCTTGTTACGACTT-3') (Palkova et al. 2021). PCR products were purified and sequenced by Nanjing General Biotech Co., Ltd. (Nanjing, China). The resulting sequences were compared against the NCBI GenBank database using BLAST to determine genus- and species-level affiliations.

2.4. In vitro antagonistic activity of phyllosphere microorganisms against N. coryli

To identify candidate biocontrol agents from the tobacco phyllosphere microbiome, we evaluated the antagonistic potential of dominant culturable bacteria and fungi against *N. coryli* YB13 through *in vitro* plate confrontation assays. For fungal-fungal interactions, mycelial plugs (5 mm diameter) were excised from the leading edge of actively growing colonies of both *N. coryli* YB13 and each test fungus. A plug of *N. coryli* YB13 was placed mycelial-side down on one side of a PDA plate, while a plug of the test fungus was positioned similarly on the opposite side, approximately 3 cm apart. Control plates consisted of a single YB13 plug inoculated at the center. All plates were incubated in the dark at 28°C. Antagonistic activity was assessed when the colony diameter of YB13 on control plates reached at least 60 mm. The nature of the interaction was observed, noting any inhibition zones or overgrowth.

For bacterial-fungal interactions, individual bacterial strains were cultured overnight in Luria-Bertani (LB) broth at 28°C with shaking at 175 rpm. Cultures were adjusted to an optical density at 600 nm (OD_{600}) of approximately 1.0. A mycelial plug of *N. coryli* YB13 was placed at the center of a fresh PDA plate. Subsequently, 5 μL aliquots of the bacterial suspension were spotted onto the agar surface at three equidistant points, each 2 cm from the central fungal plug. Control plates were inoculated with the YB13 plug only. After incubation at 28°C, antagonistic effects, such as inhibition of radial growth, were evaluated once the colony diameter on control plates exceeded 60 mm. All assays were performed with three replicates.

2.5. In planta validation of microbial interactions on disease development

To validate the biocontrol potential of selected phyllosphere microbes under conditions resembling natural infection, we assessed their ability to modulate disease severity caused by *N. coryli* YB13 on tobacco leaves via co-inoculation assays. Healthy tobacco plants (cv. Yunyan 87) at the four-to-five-leaf stage were selected for the assay. For each inoculation site, a shallow, non-penetrating

wound was made on either side of the leaf midvein using a sterile needle. A 5-mm mycelial plug of *N. coryli* YB13, taken from the margin of an actively growing colony, was placed over the wound. Plants were maintained in a controlled-environment chamber to allow infection to establish. After five days of incubation, once successful infection was confirmed by the presence of visible mycelia on the abaxial leaf surface, the original pathogen plugs were carefully and aseptically removed. They were immediately replaced with 5-mm mycelial plugs (for fungal test strains) or 5-μL aliquots of bacterial suspension (OD_{600}≈1.0, for bacterial test strains) of the phyllosphere microorganisms being evaluated. Each test strain was applied to three independent leaves (biological replicates). Two control groups were included: a positive control, where the initial *N. coryli* plug was not removed, and a negative control, consisting of wounded leaves that received no microbial inoculum. All plants were kept in the controlled-environment chamber, and lesion diameters were measured at regular intervals post-treatment to quantify disease development.

2.6. Sensitivity of N. coryli to fungicides applied singly or in mixtures

To determine the sensitivity of *N. coryli* to test fungicides alone or in mixtures, mycelial plugs (5 mm diameter) were excised from the margin of 5-day-old colonies of *N. coryli* YB13 grown on PDA. These plugs were transferred onto fresh PDA plates amended with a series of concentrations of each test fungicide. For mixture assays, the four most effective fungicides were combined at volume ratios of 4:1, 2:1, 1:1, 1:2, and 1:4, with total concentrations prepared as described in Table S3. Control plates contained no fungicide. All plates were incubated at 25°C for 7 days. Each treatment was performed in triplicate, and the entire experiment was conducted twice to ensure reproducibility. The rate of inhibition of mycelial growth = (Average diameters of control group - Average diameters of treatment group)/Average diameters of control group × 100%. For each fungicide treatment (single or in mixture), the concentration resulting in 50% inhibition of mycelial

224 growth (EC_{50}) was estimated by regressing the inhibition rate against the log-transformed
225 fungicide concentration. Regression equations and EC_{50} values were computed using Data
226 Processing System (DPS) software (Tang and Zhang 2012).

227 ***2.7. Synergistic effects of fungicides on in vitro mycelial growth***

228 As noted in the previous section, the effects of test fungicides alone and in mixtures were
229 determined for YB13. The interactive effects of the two fungicides were assessed by comparison
230 of observed and expected EC_{50} values. Observed EC_{50} values were obtained for single fungicide
231 treatments and mixtures as described in the previous section. Expected EC_{50} values for mixtures
232 were calculated as previously described using the following equation: Expected EC_{50} = (a + b) /
233 [a/EC_{50}(A) + b/EC_{50}(B)], where a and b represent the proportion of fungicides in the mixture,
234 respectively, and EC_{50}(A) and EC_{50}(B) represent the observed EC_{50} values of fungicides,
235 respectively. The synergy ratio (SR) is the ratio of the expected to the observed EC_{50} values. When
236 SR > 1.5 the interaction is defined as synergistic. When 1.5 > SR > 0.5 the interaction is defined
237 as additive. When SR < 0.5 the interaction is defined as antagonistic.

238 ***2.8. Data analysis***

239 All data are presented as the mean of three independent biological replicates ± standard error of
240 the mean (SEM). Normality of data distribution was assessed using the Shapiro–Wilk test
241 (González-Estrada et al. 2022). For datasets that conformed to normality assumptions, differences
242 among treatment groups were evaluated using one-way analysis of variance (ANOVA), followed
243 by Duncan's multiple range test for post-hoc pairwise comparisons at a significance threshold of P
244 < 0.05 (Yossa and Verdegem 2015). For datasets that deviated from normality, the non-parametric
245 Kruskal–Wallis test was applied to assess overall differences among groups (Guo et al. 2013) . All
246 statistical analyses were conducted using SPSS (version 26.0, IBM Corp., USA).

3. Results

3.1. Biological characteristics and environmental adaptability of N. coryli

To establish a foundation for predicting disease outbreaks and developing targeted control strategies, we first characterized the biological traits of *N. coryli* isolate YB13, previously confirmed as pathogenic on tobacco (Zou et al. 2026). The pathogen grows on all tested media, with PDA supporting the most vigorous vegetative growth after 14 days at 28°C, indicating it as the optimal medium for *in vitro* cultivation (Fig. 1A).

As depicted in Figure 1B, temperature strongly influenced mycelial growth expansion: growth increased from 20°C to 28°C, reaching a colony diameter of approximately 50 mm after 7 days, then declined at higher temperatures, with 57°C identified as the lethal temperature (Fig. 1B, G). Additionally, *N. coryli* YB13 exhibits broad pH tolerance, growing across pH 4-11, with optimal growth at pH 6.0 (Fig. 1C). Light also promotes growth, with maximal colony diameters under constant light (Fig. 1D). Nutritional profiling revealed that soluble starch and peptone are the preferred carbon and nitrogen sources, respectively (Fig. 1E, F). Collectively, these results highlight the robust adaptability of *N. coryli*, providing key insights into environmental factors that may influence disease development.

3.2. Phyllosphere microbial community dynamics during infection

High-throughput sequencing revealed the *N. coryli* infection substantially reshaped the tobacco phyllosphere microbiome. A total of 334,621 high-quality sequences yielded 240 ASVs for downstream analysis (Table S2). In asymptomatic leaves, Cyanobacteria dominated bacterial communities (89.65%), while Proteobacteria and Bacteroidota were enriched in symptomatic tissue (41.75% and 4.48%) (Fig. 2A). At the genus level, *Pseudomonas* and *Chryseobacterium*

declined, suggesting disease-induced shifts that may favor opportunistic taxa ot reflect native antagonistic responses (Fig. 2B).

Fungal communities were dominated by *Ascomycota*, which increased from 0.25% in healthy leaves to 8.40% in diseased tissue. At the genus level, *Nigrospora* and *Sarocladium* were detected exclusively in symptomatic leaves, with relative abundances of 5.15% and 3.21%, respectively (Fig. 2C, D). Venn diagrams analysis showed that only 23.44% of bacterial ASVs and 32.26% of fungal ASVs were shared between healthy and diseased leaves, highlighting substantial microbiome restructuring during disease progression (Fig. 2E and 2F). These findings indicate that *N. coryli* infection creates new microbial niches, some of which may harbor potential biocontrol agents.

3.3. Antagonistic interactions of phyllosphere microorganisms

To explore the functional potential of these microbiome shifts, we isolated dominant microbial strains from symptomatic leaves and evaluated their antagonistic activity against *N. coryli* in vitro. Among bacteria, *Bacillus halotolerans* TBX4 and *Pseudomonas oryzihabitan* SLB2-1 strongly inhibited mycelial growth, whereas *Pseudomonas syringae* pv. *angulata* SLB-5-3 had negligible effect (Fig. 3A).

Among fungi, isolates including *Alternaria alternata* CXB, *Epicoccum latusicollum* CMB1-2-1, *Corynespora cassiicola* WZ45, *Fusarium oxysporum* ZY14, *Aspergillus niger* MGM and ZYO1, and *Fusarium nelsonii* HB exhibited near-complete inhibition of *N. coryli* growth (Fig. 3B), likely through competition for space and nutrients or secretion of antifungal compounds. These results identified a shortlist of microbial candidates for potential biocontrol applications.

3.4. In planta validation of microbial antagonism

To confirm the *in vitro* findings under conditions resembling natural infection, representative fungal and bacterial isolates were co-inoculated with *N. coryli* on tobacco leaves. Co-inoculation with the five strongly antagonistic fungi significantly reduced lesion size compared to the pathogen-only control, with *A. niger* MGM achieving an 87.60% reduction (lesion diameter: 0.88 mm vs. 7.11 mm) (Fig. 4, Table 1). In contrast, *P. syringae* pv. *angulata* SLB-5-3 increased lesion size, highlighting that some phyllosphere bacteria may exacerbate disease. These results demonstrate the practical potential of selected fungal isolates as biocontrol agents and underscore the importance of considering both beneficial and detrimental microbial interactions in disease management.

3.5. Chemical control and fungicide efficacy

Eight commercially available fungicides were evaluated against *N. coryli* YB13 at 1 μg/mL. These fungicides, selected based on their documented efficacy against *Nigrospora* species and their widespread use in managing leaf spot and other diseases in tobacco production (Guarnaccia et al. 2014; Koehler and Shew 2018; Duan et al. 2019; García et al. 2023). Fludioxonil exhibited complete inhibition (100%), followed by the prochloraz-manganese chloride complex (80%), fenaminstrobin (75.45%), and difenoconazole (61.82%) (Table 2). Dose-response assay confirmed fludioxonil as the most potent compound (EC_{50} = 0.0057 μg/mL), followed by the prochloraz-manganese chloride complex (0.0160 μg/mL), difenoconazole (0.0463 μg/mL), and fenaminstrobin (0.0757 μg/mL) (Table 3).

3.6. Synergistic effects of fungicide combinations

To improve application efficiency and delay resistance, binary mixtures of the four most effective fungicides were assessed. Synergistic inhibition (SR > 1.5) was observed for fludioxonil + difenoconazole (1:4, SR = 1.7360), fludioxonil + fenaminstrobin (1:1, SR = 1.5365), and

difenoconazole + fenaminstrobin (1:2, SR = 2.0219) (Tables 5–7). Other combinations displayed additive effects ($0.5 \leq SR \leq 1.5$). These results identify promising fungicide mixture that pair distinct modes of action to enhance efficacy and mitigate resistance development.

Discussion

Widespread leaf spot disease caused by fungal pathogens can severely reduce tobacco yield and quality, resulting in economic losses worldwide (Gonzalez et al. 2010). Among these pathogens, *Nigrospora* species have emerged as major threats to economically important crops (Hao et al. 2020). In China, *N. coryli* was recently identified as a novel causal agent of leaf spot (Zou et al. 2026), yet its biology, ecological interactions, and management strategies remained largely unexplored. This study provides a comprehensive characterization of *N. coryli*, integrating growth physiology, phyllosphere microbial community shifts, microbial interactions, and fungicide sensitivity, offering a foundation for sustainable integrated management.

N. coryli displayed strong environmental adaptability, with optimal growth on PDA at 28°C and pH 6.0, tolerance to a wide pH range (4-11), and high-temperature resilience up to 57°C. Such versatility enables the pathogen to survive under diverse field conditions, limiting the efficacy of cultural control alone. Its preference for soluble starch and peptone as carbon and nitrogen sources reflects adaptation to complex plant-derived nutrients, likely contributing to pathogenic fitness and host adaptability, consistent with observations in other *Nigrospora* species (Hao et al. 2020; Orina et al. 2023).

Phyllosphere microbiome analysis revealed substantial compositional shifts during disease. *Stenotrophomonas* and *Pseudomonas* were enriched in symptomatic leaves, while *Nigrospora* and *Sarocladium* were detected exclusively in disease tissue, confirming the pathogen's role and potential secondary colonization or synergistic interactions (Sun et al. 2017; Kumar et al. 2023;

Nakagami et al. 2024). Similar shifts in microbial community structure have been reported in tobacco leaves infected by other fungal pathogens (Xiang et al. 2022a; Xiang et al. 2022b; Guo et al. 2024), indicating that pathogen invasion creates distinct ecological niches that selectively favor specific microbial taxa. These shifts highlight the dynamic nature of microbial communities in response to infection and support the use of phyllosphere profiling to identify candidate biocontrol agents.

Multiple fungi from symptomatic leaves exhibited strong antagonism against *N. coryli* in vitro and in planta. Notably, *A. niger* MGM reduced lesion size by 87.60%, likely through competitive exclusion and antifungal metabolite production (Hu et al. 2022; Nguyen et al. 2022). The coexistence of multiple fungi in diseased tissues underscores that the phyllosphere is a dynamic microenvironment where microbial competition influences disease outcomes. Conversely, *P. syringae* pv. a*ngulata* SLB-5-3 exacerbated disease, highlighting that some bacteria may facilitate infection or suppress host defense. Bacterial strains with strong *in vitro* inhibition, such as *B. halotolerans* TBX4 and *P. oryzihabitan* SLB2-1, merit further investigation.

Chemical control assay identified fludioxonil as the most potent fungicide (EC_{50} = 0.0057 μg/mL), followed by the prochloraz-manganese chloride complex, difenoconazole, and fenaminstrobin, representing diverse chemical classes and modes of action. Binary mixtures combining fungicides from different FRAC groups demonstrated synergistic effects: fludioxonil + difenoconazole (1:4, SR = 1.7360), fludioxonil + fenaminstrobin (1:1, SR = 1.5365), and difenoconazole + fenaminstrobin (1:2, SR = 2.0219). These combinations enhance efficacy, reduce chemical inputs, and mitigate resistance development by targeting multiple cellular pathways, consistent with strategies effective against *Fusarium graminearum* and *Nothopassalora personata* (Paul et al. 2018; Culbreath et al. 2020).

The integration of biological and chemical control approaches offers a promising avenue for sustainable management. Biocontrol agents, particularly *A. niger* MGM, could be applied alongside reduced rates of synergistic fungicide mixtures to achieve effective disease suppression while preserving beneficial phyllosphere microbiota. Such integrated approaches align with the principles of sustainable agriculture and have been successfully implemented for other pathosystems (Zhou et al. 2021). Future studies should evaluate field efficacy, compatibility, and mechanistic interactions of these integrated strategies to optimize practical deployment in tobacco cultivation.

In summary, this study establishes the biology of *N. coryli*, microbial interactions, and chemical control options. The pathogen's broad environmental tolerance, coupled with disease-associated microbiome restructuring, underscores the need for integrated management strategies. The identification of potent fungal biocontrol agents and synergistic fungicide combinations provides a scientific foundation for multifaceted, sustainable control of *Nigrospora*-induced tobacco leaf spot in China and beyond.

Acknowledgements

This work is supported by China National Tobacco Corporation (110202101048(LS-08)), Key Research and Development Program of Hainan Province (ZDYF2023XDNY034), Jiangsu Provincial Basic Research Special Fund for Soft Science Research (BZ2024056), Guizhou Science Technology Foundation (Qiankehe Talent Platform – CXTD[2023]021), "Hundred" Level Innovative Talent Foundation of Guizhou Province (GCC[2022]028–2, GCC[2023]108), National Natural Science Foundation of China (32460698), Guizhou Tobacco Company Project (2024XM06) and National Key Research and Development Program of China (2022YFD1700300 and 2022YFD1700200).

CRediT authorship contribution statement

Jingpei Zou: Writing – original draft, Methodology, Investigation, Formal analysis. **Liuti Cai:** Methodology, Investigation, Formal analysis. **Yiming Geng:** Investigation, Formal analysis. **Mengyu Yin:** Investigation. **Yuguang Mu:** Software, Resources. **Jingjing Guo:** Formal analysis. **Hancheng Wang:** Writing – review & editing, Supervision, Project administration, Funding acquisition. **Feng Zhang:** Writing – review & editing, Supervision, Project administration, Funding acquisition, Conceptualization.

Declaration of Competing Interest

The authors declare no conflicts of interests.

References

Abarenkov K et al. (2024) The UNITE database for molecular identification and taxonomic communication of fungi and other eukaryotes: sequences, taxa and classifications reconsidered. Nucleic Acids Research 52:D791-D797 doi: 10.1093/nar/gkad1039

Bolyen E et al. (2019) Reproducible, interactive, scalable and extensible microbiome data science using QIIME 2. Nature Biotechnology 37:852-857 doi: 10.1038/s41587-019-0209-9

Callahan BJ, McMurdie PJ, Rosen MJ, Han AW, Johnson AJA, Holmes SP (2016) DADA2: High-resolution sample inference from Illumina amplicon data. Nature Methods 13:581-583 doi: 10.1038/nmeth.3869

Chen Q et al. (2022) Genera of phytopathogenic fungi: GOPHY 4. Studies in Mycology 101:417-564 doi: 10.3114/sim.2022.101.06

Chuvochina M et al. (2026) SILVA in 2026: a global core biodata resource for rRNA within the DSMZ digital diversity. Nucleic Acids Research 54:D334-D341 doi: 10.1093/nar/gkaf1247

Clarke JD (2009) Cetyltrimethyl Ammonium Bromide (CTAB) DNA Miniprep for Plant DNA Isolation. Cold Spring Harbor Protocols 2009:pdb-prot5177 doi: 10.1101/pdb.prot5177

Culbreath AK, Brenneman TB, Kemerait RC, Stevenson KL, Henn A (2020) Effect of DMI and QoI fungicides mixed with the SDHI fungicide penthiopyrad on late leaf spot of peanut. Crop Protection 137 doi: 10.1016/j.cropro.2020.105298

De Wolf ED, Isard SA (2007) Disease Cycle Approach to Plant Disease Prediction. Annual Review of Phytopathology 45:203-220 doi: 10.1146/annurev.phyto.44.070505.143329

Duan Y et al. (2019) Benzimidazole- and QoI-resistance in *Corynespora cassiicola* populations from greenhouse-cultivated cucumber: an emerging problem in China.

Pesticide Biochemistry and Physiology 153:95-105 doi: 10.1016/j.pestbp.2018.11.006
Feng R et al. (2024) Characteristics of *Corynespora cassiicola*, the causal agent of tobacco *Corynespora* leaf spot, revealed by genomic and metabolic phenomic analysis. Scientific Reports 14:18326 doi: 10.1038/s41598-024-67510-y
García JLM, Hernández MDSM, Miguel EE, Montelongo KLM (2023) Isolation, identification and *in vitro* chemical control of pathogens related to RoÑa syndrome in avocado. Journal of Agricultural Sciences Research (2764-0973) 3:2-11 doi: 10.22533/at.ed.973372330058
González-Estrada E, Villaseñor JA, Acosta-Pech R (2022) Shapiro-Wilk test for multivariate skew-normality. Computational Statistics 37:1985-2001 doi: 10.1007/s00180-021-01188-y
Gonzalez M, Pujol M, Metraux JP, Gonzalez‐Garcia V, Bolton MD, BorrÁS‐Hidalgo O (2010) Tobacco leaf spot and root rot caused by *Rhizoctonia solani* Kühn. Molecular Plant Pathology 12:209-216 doi: 10.1111/j.1364-3703.2010.00664.x
Guarnaccia V, Aiello D, Polizzi G, Perrone G, Stea G, Vitale A (2014) Emergence of Prochloraz-Resistant Populations of *Calonectria pauciramosa* and *Calonectria polizzii* in Ornamental Nurseries of Southern Italy. Plant Disease 98:344-350 doi: 10.1094/Pdis-04-13-0425-Re
Gui Z-Q, Yuan X-L, Yang J, Du Y-M, Zhang P (2024) An updated review on chemical constituents from *Nicotiana tabacum* L.: Chemical diversity and pharmacological properties. Industrial Crops and Products 214:118497 doi: 10.1016/j.indcrop.2024.118497
Guo M et al. (2024) Response of microbial communities in the tobacco phyllosphere under the stress of validamycin. Frontiers in Microbiology 14:1328179 doi: 10.3389/fmicb.2023.1328179
Guo S, Zhong S, Zhang A (2013) Privacy-preserving Kruskal–Wallis test. Computer Methods and Programs in Biomedicine 112:135-145 doi: 10.1016/j.cmpb.2013.05.023
Hao Y et al. (2020) *Nigrospora* species associated with various hosts from Shandong Peninsula, China. Mycobiology 48:169-183 doi: 10.1080/12298093.2020.1761747
Hu Z et al. (2022) Sesquiterpenoids with phytotoxic and antifungal activities from a pathogenic fungus *Aspergillus alabamensis*. Journal of Agricultural and Food Chemistry 70:12065-12073 doi: 10.1021/acs.jafc.2c05703
Huang C et al. (2025) Biocontrol efficacy of YZU 173039 against *Corynespora* leaf spot on tobacco. Biocontrol Science and Technology 35:527-540 doi: 10.1080/09583157.2025.2481506
Huang Y, Li Z, Wang H, Chen Q, Li W (2021) First report of leaf spot caused by *Nigrospora aurantiaca* in tobacco in China. Plant Disease 105:1569 doi: 10.1094/pdis-06-20-1201-pdn
Koehler AM, Shew HD (2018) Field efficacy and baseline sensitivity of Septoria steviae to fungicides used for managing Septoria leaf spot of stevia. Crop Protection 109:95-101 doi: 10.1016/j.cropro.2018.03.006
Kumar A et al. (2023) Stenotrophomonas in diversified cropping systems: friend or foe? Frontiers in Microbiology 14 doi: 10.3389/fmicb.2023.1214680

Le Foll B et al. (2022) Tobacco and nicotine use. Nature Reviews Disease Primers 8:19 doi: 10.1038/s41572-022-00346-w
Luo M-Y, Jiang Y-L (2022) First report of leaf spot on kidney bean caused by *Nigrospora oryzae* in China. Plant Disease 106:1064 doi: 10.1094/pdis-06-21-1171-pdn
Martins-da-Silva AS et al. (2022) Tobacco growing and tobacco use. International Review of Psychiatry 34:51-58 doi: 10.1080/09540261.2022.2034602
Nakagami S, Wang Z, Han X, Tsuda K (2024) Regulation of Bacterial Growth and Behavior by Host Plant. Annual Review of Phytopathology 62:69-96 doi: 10.1146/annurev-phyto-010824-023359
Nguyen MV, Han JW, Kim H, Choi GJ (2022) Phenyl ethers from the marine-derived fungus *Aspergillus tabacinus* and their antimicrobial activity against plant pathogenic fungi and bacteria. ACS Omega 7:33273-33279 doi: 10.1021/acsomega.2c03859
O'Brien HE, Parrent JL, Jackson JA, Moncalvo J-M, Vilgalys R (2005) Fungal Community Analysis by Large-Scale Sequencing of Environmental Samples. Applied and Environmental Microbiology 71:5544-5550 doi: 10.1128/aem.71.9.5544-5550.2005
Ons L, Bylemans D, Thevissen K, Cammue BPA (2020) Combining biocontrol agents with chemical fungicides for integrated plant fungal disease control. Microorganisms 8:1930 doi: 10.3390/microorganisms8121930
Orina AS, Gavrilova OP, Gagkaeva TY (2023) Physiological and biochemical characters of *Nigrospora gorlenkoana* novobr. occurring on cereals. Biology Bulletin 50:837-849 doi: 10.1134/s1062359023602550
Palkova L et al. (2021) Evaluation of 16S rRNA primer sets for characterisation of microbiota in paediatric patients with autism spectrum disorder. Scientific Reports 11 doi: 10.1038/s41598-021-86378-w
Paul PA et al. (2018) Meta-Analysis of the Effects of QoI and DMI Fungicide Combinations on Fusarium Head Blight and Deoxynivalenol in Wheat. Plant Disease 102:2602-2615 doi: 10.1094/pdis-02-18-0211-re
Shi S, Kumar S, Young S, Maclean P, Jauregui R (2023) Evaluation of 16S rRNA gene primer pairs for bacterial community profiling in an across soil and ryegrass plant study. Journal of Sustainable Agriculture and Environment 2:500-512 doi: 10.1002/sae2.12075
Stone BWG, Weingarten EA, Jackson CR (2018) The role of the phyllosphere microbiome in plant health and function. In: Annual Plant Reviews, pp 533-556
Sun D, Zhuo T, Hu X, Fan X, Zou H (2017) Identification of a Pseudomonas putida as biocontrol agent for tomato bacterial wilt disease. Biological Control 114:45-50 doi: 10.1016/j.biocontrol.2017.07.015
Tang QY, Zhang CX (2012) Data Processing System (DPS) software with experimental design, statistical analysis and data mining developed for use in entomological research. Insect Science 20:254-260 doi: 10.1111/j.1744-7917.2012.01519.x
Tao Y, Yang C, Yu S, Fu F, Dai T (2024) New Occurrence of *Nigrospora oryzae* Causing Leaf Blight in *Ginkgo biloba* in China and Biocontrol Screening of Endophytic Bacteria. Microorganisms 12:2125 doi: 10.3390/microorganisms12112125
Wang M, Liu F, Crous PW, Cai L (2017) Phylogenetic reassessment of *Nigrospora*: ubiquitous endophytes, plant and human pathogens. Persoonia - Molecular Phylogeny and Evolution of Fungi 39:118-142 doi: 10.3767/persoonia.2017.39.06

Warner KE (2000) The economics of tobacco: myths and realities. Tobacco Control 9:78-89 doi: DOI 10.1136/tc.9.1.78

Xiang L-G et al. (2022a) Variations in leaf phyllosphere microbial communities and development of tobacco brown spot before and after fungicide application. Frontiers in Microbiology 13 doi: 10.3389/fmicb.2022.1068158

Xiang L-G et al. (2022b) Analysis of phyllosphere microorganisms and potential pathogens of tobacco leaves. Frontiers in Microbiology 13 doi: 10.3389/fmicb.2022.843389

Xu T et al. (2022) Secondary metabolites of the genus *Nigrospora* from terrestrial and marine habitats: chemical diversity and biological activity. Fitoterapia 161:105254 doi: 10.1016/j.fitote.2022.105254

Yossa R, Verdegem M (2015) Misuse of multiple comparison tests and underuse of contrast procedures in aquaculture publications. Aquaculture 437:344-350 doi: 10.1016/j.aquaculture.2014.12.023

Zhou X-G, Kumar KVK, Zhou LW, Reddy MS, Kloepper JW (2021) Combined use of PGPRs and reduced rates of azoxystrobin to improve management of sheath blight of rice. Plant Disease 105:1034-1041 doi: 10.1094/pdis-07-20-1596-re

Zou J et al. (2026) First Report of Leaf Spot Caused by *Nigrospora coryli* on Tobacco in China. Plant Disease (ja):DOI: 10.1094/pdis-1012-1025-2552-pdn doi: 10.1094/pdis-12-25-2552-pdn

Figures and Tables

Table 1

Effects of co-inoculation with dominant phyllosphere bacteria and fungi on lesion development caused by *N. coryli* YB13.

Reciprocal strain	Lesion Diameter (mm)		
	***N. coryli* YB13**	**Monoinfection**	**Co-infection**
A. alternata CXB	7.11 ± 0.45	0.00 ± 0.00	3.30 ± 0.38
E. latusicollum CMB1-2-1		0.00 ± 0.00	1.53 ± 0.21
C. cassiicola WZ45		2.22 ± 0.31	3.63 ± 0.42
F. oxysporum ZY14		9.72 ± 0.67	5.05 ± 0.44
A. niger MGM		9.84 ± 0.71	0.88 ± 0.12
P. syringae pv. angulata SLB-5-3		4.30 ± 0.36	16.55 ± 1.23

Data are presented as mean ± standard error (SE) of three biological replicates.

Table 2

Inhibition of mycelial growth of *N. coryli* YB13 by eight fungicides at 1 μg/mL.

Fungicide	Concentration (μg/mL)	Inhibition rate (%)
Fludioxonil	1	100.00 ± 0.00
Prochloraz-manganese chloride complex	1	80.00 ± 1.81
Difenoconazole	1	61.82 ± 2.25
Fenaminstrobin	1	75.45 ± 0.87
Epoxiconazole	1	57.27 ± 1.11
Cyazofamid	1	45.45 ± 1.23
Azoxystrobin	1	19.09 ± 0.75
Trifloxystrobin	1	19.09 ± 2.62

Data are presented as mean ± standard error (SE) of three biological replicates.

Table 3

Toxicity of four fungicides against *N. coryli* YB13.

Fungicide	Linear regression equation	R^2	EC_{50} (μg/mL)
Fludioxonil	Y=7.1703+0.9668X	0.9921	0.0057
Prochloraz-manganese chloride complex	Y=6.9698+1.0966X	0.9933	0.0160
Difenoconazole	Y=5.7010+0.5254X	0.9963	0.0463
Fenaminstrobin	Y=5.2670+0.2383X	0.9905	0.0757

539

540 **Table 4**

541 Interactions between fludioxonil and prochloraz-manganese chloride complex based on

542 inhibition of myceilal growth of *N. coryli* YB13.

Fungicide	Linear regression equation	R^2	Observed EC_{50} (μg/mL)	Expected EC_{50} (μg/mL)	Synergy ratio[z] (SR)
Fludioxonil	Y=7.1703+0.9668X	0.9921	0.0057		
Prochloraz-manganese chloride complex	Y=6.9698+1.0966X	0.9933	0.0160		
Fludioxonil:Prochloraz-manganese chloride complex (4:1)	Y=7.6790+1.3131X	0.9980	0.0091	0.0065	0.7143
Fludioxonil:Prochloraz-manganese chloride complex (2:1)	Y=6.9263+0.9702X	0.9956	0.0103	0.0073	0.7087
Fludioxonil:Prochloraz-manganese chloride complex (1:1)	Y=7.0473+0.9559X	0.9851	0.0072	0.0084	1.1667

Fludioxonil:Prochloraz-manganese chloride complex (1:2)	Y=7.4399+1.2036X	0.9952	0.0094	0.0100	1.0638
Fludioxonil:Prochloraz-manganese chloride complex (1:4)	Y=6.9721+1.0807X	0.9889	0.0150	0.0118	0.7867

[Z] Ratio between expected and observed EC_{50} values.

Table 5

Interactions between fludioxonil and difenoconazole based on inhibition of myceilal growth of *N. coryli* YB13.

Fungicide	**Linear regression equation**	**R^2**	**Observed EC_{50} (μg/mL)**	**Expected EC_{50} (μg/mL)**	**Synergy ratio[z] (SR)**
Fludioxonil	Y=7.1703+0.9668X	0.9921	0.0057		
Difenoconazole	Y=5.7010+0.5254X	0.9963	0.0463		
Fludioxonil:Difenoconazole (4:1)	Y=7.7850+1.2448X	0.9966	0.0058	0.0069	1.1918
Fludioxonil:Difenoconazole (2:1)	Y=7.7452+1.2577X	0.9816	0.0066	0.0081	1.2203
Fludioxonil:Difenoconazole (1:1)	Y=7.2015+1.0552X	0.9966	0.0082	0.0102	1.2379
Fludioxonil:Difenoconazole (1:2)	Y=7.1740+1.1087X	0.9827	0.0109	0.0137	1.2589
Fludioxonil:Difenoconazole (1:4)	Y=6.9926+1.0176X	0.9880	0.0110	0.0191	1.7360

548 [Z] Ratio between expected and observed EC_{50} values.

549

550 **Table 6**

551 Interactions between fludioxonil and fenaminstrobin based on inhibition of myceilal growth of

552 *N. coryli* YB13.

Fungicide	Linear regression equation	R^2	Observed EC_{50} (μg/mL)	Expected EC_{50} (μg/mL)	Synergy ratio[z] (SR)
Fludioxonil	Y=7.1703+0.9668X	0.9921	0.0057		
Fenaminstrobin	Y=5.2670+0.2383X	0.9905	0.0757		
Fludioxonil:Fenaminstrobin (4:1)	Y=7.6821+1.1550X	0.9904	0.0048	0.0070	1.4569
Fludioxonil:Fenaminstrobin (2:1)	Y=8.5140+1.7492X	0.9901	0.0098	0.0082	0.8408
Fludioxonil:Fenaminstrobin (1:1)	Y=8.0780+1.4232X	0.9862	0.0069	0.0106	1.5365
Fludioxonil:Fenaminstrobin (1:2)	Y=6.9030+0.9789X	0.9925	0.0114	0.0149	1.3037
Fludioxonil:Fenaminstrobin (1:4)	Y=5.5911+0.3968X	0.9936	0.0324	0.0219	0.6760

553 [Z] Ratio between expected and observed EC_{50} values.

554

555 **Table 7**

556 Interactions between difenoconazole and fenaminstrobin based on inhibition of myceilal growth

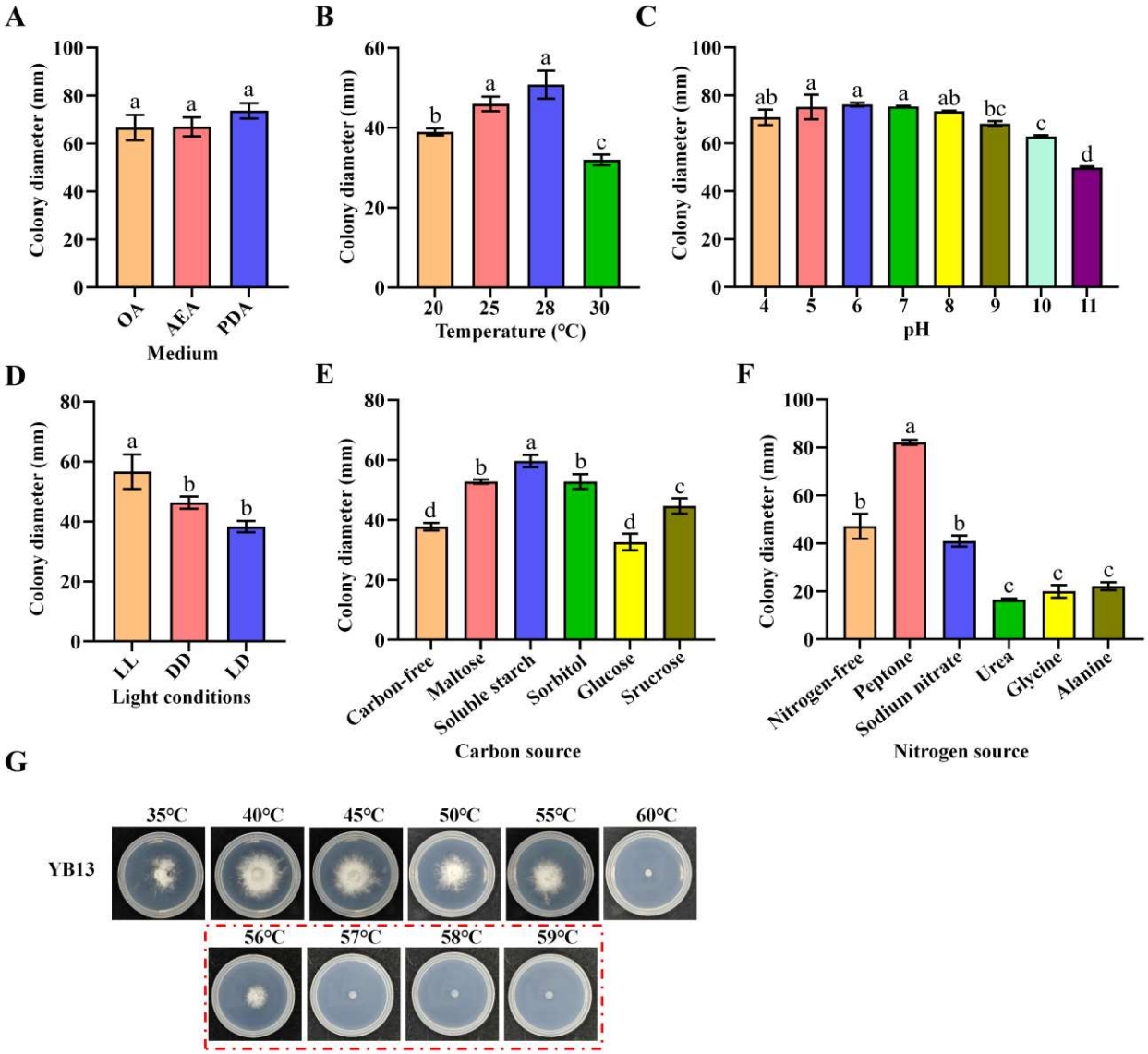
557 of *N. coryli* YB13.

Fungicide	Linear regression equation	R^2	Observed EC_{50} (μg/mL)	Expected EC_{50} (μg/mL)	Synergy ratio[z] (SR)
Difenoconazole	Y=5.7010+0.5254X	0.9963	0.0463		
Fenaminstrobin	Y=5.2670+0.2383X	0.9905	0.0757		
Difenoconazole:Fenaminstrobin (4:1)	Y=6.0185+0.8082X	0.9956	0.0549	0.0502	0.9144
Difenoconazole:Fenaminstrobin (2:1)	Y=5.9629+0.7430X	0.9814	0.0506	0.0532	1.0511
Difenoconazole:Fenaminstrobin (1:1)	Y=5.8242+0.5894X	0.9948	0.0400	0.0575	1.4364
Difenoconazole:Fenaminstrobin (1:2)	Y=6.0644+0.7051X	0.9964	0.0309	0.0625	2.0219
Difenoconazole:Fenaminstrobin (1:4)	Y=5.7286+0.5413X	0.9834	0.0451	0.0672	1.4893

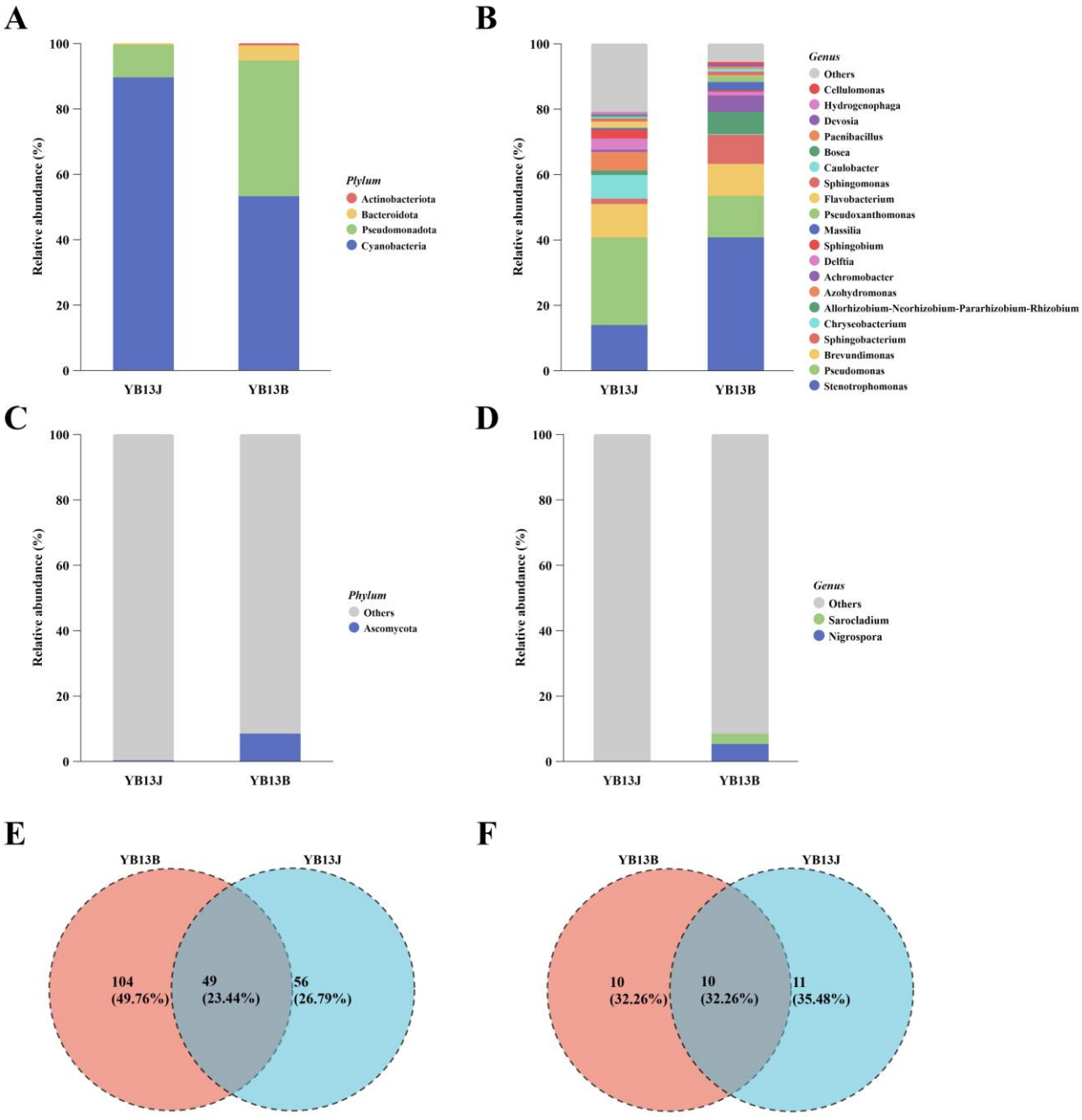
[z] Ratio between expected and observed EC_{50} values.

Fig. 1. Biological characteristics of *N. coryli* YB13 under various environmental conditions. (A) Colony diameters on different media after 14 days of incubation at 28°C; (B) Colony diameters at different temperatures after 7 days of incubation; (C) Colony diameters at different pH levels after 14 days of incubation at 28°C; (D) Colony diameters under different light regimes after 14 days of incubation at 28°C; (E) Colony diameters on different carbon sources after 7 days of incubation at 28°C; (F) Colony diameters on different nitrogen sources after 7 days of incubation at 28°C; (G) Mycelial growth after exposure to different temperatures for 10 min followed by 7 days of incubation at 28°C. Values represent the mean ± standard error (SE) of three biological

replicates. Different lowercase letters above bars indicate statistically significant differences among treatments (one-way ANOVA followed by LSD test, $P < 0.05$).



572 **Fig.2.** Microbial community composition and diversity in asymptomatic (YB13J) and
573 symptomatic (YB13B) tobacco leaves. (A) Bacterial community composition at the phylum level;
574 (B) Bacterial community composition at the genus level; (C) Fungal community composition at
575 the phylum level; (D) Fungal community composition at the genus level; (E) Venn diagram
576 showing shared and unique bacterial ASVs between asymptomatic and symptomatic leaves; (F)
577 Venn diagram showing shared and unique fungal ASVs between asymptomatic and symptomatic
578 leaves.
579


A
Relative abundance (%)
100
80
60
40
20
0
YB13J
YB13B
Plylum
Actinobacteriota
Bacteroidota
Pseudomonadota
Cyanobacteria
B
Relative abundance (%)
YB13J
YB13B
Genus
Others
Cellulomonas
Hydrogenophaga
Devosia
Paenibacillus
Bosea
Caulobacter
Sphingomonas
Flavobacterium
Pseudoxanthomonas
Massilia
Sphingobium
Delftia
Achromobacter
Azohydromonas
Allorhizobium-Neorhizobium-Pararhizobium-Rhizobium
Chryseobacterium
Sphingobacterium
Brevundimonas
Pseudomonas
Stenotrophomonas
C
Relative abundance (%)
YB13J
YB13B
Phylum
Others
Ascomycota
D
Relative abundance (%)
YB13J
YB13B
Genus
Others
Sarocladium
Nigrospora
E
YB13B
YB13J
104
(49.76%)
49
(23.44%)
56
(26.79%)
F
YB13B
YB13J
10
(32.26%)
10
(32.26%)
11
(35.48%)

580

581

Fig.3. *In vitro* antagonistic activity of phyllosphere microorganisms against *N. coryli* YB13 in plate confrontation assays. (A) Bacterial strains tested: *Bacillus halotolerans* TBX4, *Pseudomonas oryzihabitan* SLB2-1, and *Pseudomonas syringae pv. angulata* SLB-5-3. (B) Fungal strains tested: *Alternaria alternata* CXB, *Epicoccum latusicollum* CMB1-2-1, *Corynespora cassiicola* WZ45, *Fusarium oxysporum* ZY14, *Aspergillus niger* MGM, *A. niger* ZYO1, *Fusarium nelsonii* HB, *Nigrospora oryzae* ZYX7, *Pestalotiopsis microspora* ZYX2, *Stemphylium lycopersici* ZYO2, *Penicillium citrinum* ZYX8, and *Pseudothielavia terricola* ZY18.

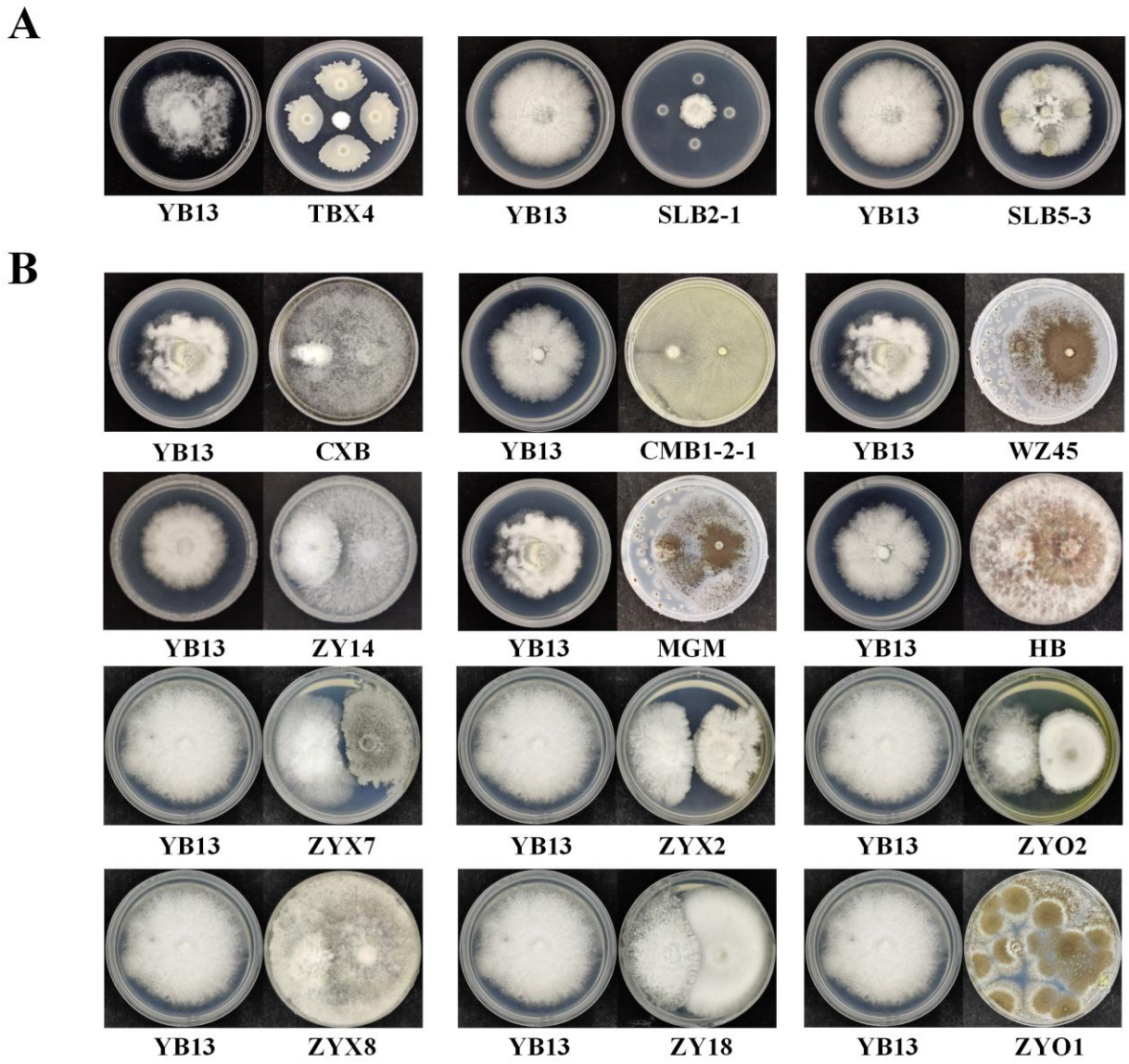
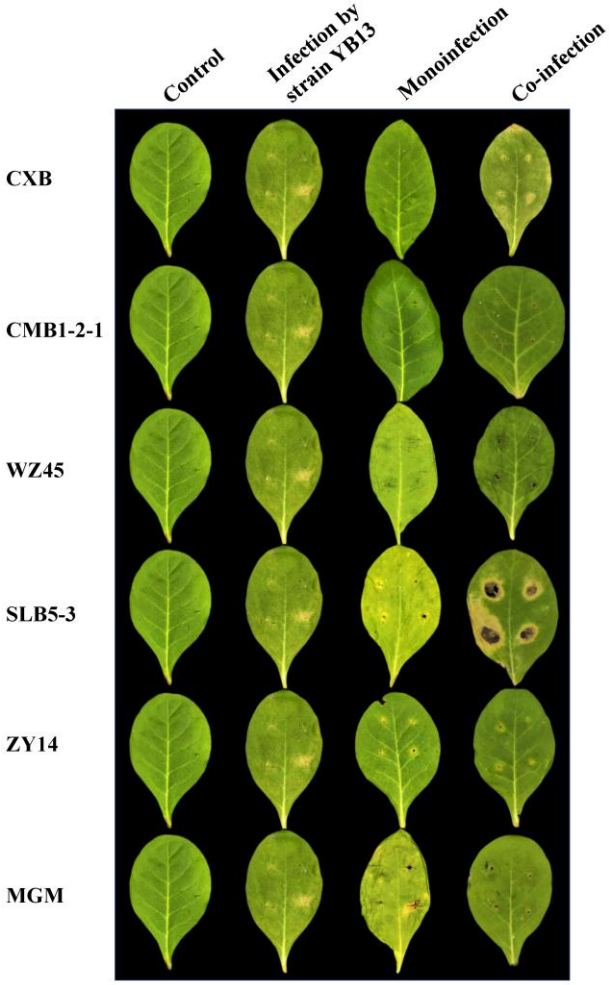


Fig.4. *In planta* validation of microbial interactions on disease development caused by *N. coryli* YB13. Leaves were pre-inoculated with *N. coryli* YB13 for five days, after which the pathogen plugs were removed and replaced with test microbial strains. (A) Bacterial strain tested: *P. syringae pv. angulata* SLB-5-3. (B) Fungal strains tested: *A. alternata* CXB, *E. latusicollum* CMB1-2-1, *C. cassiicola* WZ45, *F. oxysporum* ZY14, and *A. niger* MGM. Control leaves were inoculated with *N. coryli* YB13 alone (positive control) or wounded without inoculation (negative control).



Supplementary Files

This is a list of supplementary files associated with this preprint. Click to download.

- SupplementaryMaterial.docx